Available online at www.sciencedirect.com
SCIENCE DIRECT®
ELSEVIER
European Journal of Mechanics B/Fluids 23 (2004) 89–97
EUROPEAN JOURNAL OF MECHANICS B/FLUIDS

Wake states and response branches of forced and freely oscillating cylinders

J. Carberry [a,*], R. Govardhan [b], J. Sheridan [a], D. Rockwell [c], C.H.K. Williamson [b]

[a] *Department of Mechanical Engineering, Monash University, Victoria 3800, Australia*
[b] *Sibley School of Mechanical and Aerospace Engineering, Upson Hall, Cornell University, Ithaca, NY, USA*
[c] *Dept. Mechanical Engineering and Mechanics, Lehigh University, Bethlehem, PA, USA*

Received 11 April 2003; accepted 16 May 2003

Abstract

A freely-oscillating, elastically-mounted cylinder has two or three different response branches, where the third response branch is characterised by high amplitude oscillations and occurs at low values of the mass-damping parameter. Similarly, a cylinder undergoing forced transverse oscillations in a free stream flow exhibits two different wake states, with an additional third state at high oscillation amplitudes. In this paper the characteristic lift properties and patterns of near wake vorticity for the forced wake states are compared with those of the free response branches. The forced oscillations are shown to replicate many features of the freely oscillating case. However, these results also show that there are some important aspects to be resolved before forced oscillations can be used to predict flow-induced motion.

Keywords: Flow induced vibrations; Vortex induced vibrations; Bluff body wakes

1. Introduction

Vortex-induced vibrations typically occur when flow past a body induces a wake whose natural frequency approaches the natural structural frequency of the body. The vortex-induced motion and the wake of the oscillating body are intrinsically interdependent; thus the relationship between these two factors is complicated and difficult to determine. This paper considers the case of a rigid cylindrical body oscillating transverse to the flow, however many of the results are relevant to non-cylindrical bluff bodies.

The early study by Feng [1] showed that an elastically-mounted freely-oscillating cylinder exhibits a range of responses depending on a number of parameters including the flow velocity U, the non-dimensional mass m^*, the non-dimensional damping ζ, and the natural frequency of the cylinder and its supporting structure f_N. A number of studies, including the recent investigation of Govardhan and Williamson [2], have examined the changes in the response in terms of the vorticity structure of the near wake and the lift forces on the cylinder. An approach to further understanding the fluid–structure interaction is to control the motion of the body, allowing the response of the wake to the motion to be examined in isolation. The response of the cylinder wake to forced motion has been extensively studied and there is a considerable body of literature describing the structure of the near wake and the forces on the cylinder, [3–5].

The relationship between the forced and freely oscillating cases, in particular the potential of the forced results to provide insight into the the more complicated freely oscillating case, is of significant interest. If the forced motion captures the "essential features" of the flow-induced motion the results of the forced oscillations can be used to predict the motion of an elastically-

* Corresponding author.
E-mail address: Josie.Carberry@bme.gatech.edu (J. Carberry).

0997-7546/$ – see front matter
doi:10.1016/j.euromechflu.2003.05.007

mounted body. Historically, the relevance of forced oscillation experiments to a wide range of engineering problems was predicated on the assumption that the flow-induced motion could be adequately represented by sinusoidal oscillations, typically at a constant oscillation amplitude and frequency. However, the links between the forced and freely oscillating cases have not been conclusively established. The prediction of flow-induced motion using the results of forced oscillation experiments was considered by Staubli [6]; otherwise, this problem has received relatively little attention. In this paper results of experiments on both forced and freely oscillating cylinders will be presented. The two cases are compared using characteristic wake structures and force properties, and the implications for the prediction of flow-induced motion are discussed.

Flow-induced motion occurs over a range of normalised free-stream velocities, $U^* = U/f_N D$, typically within the region where the natural Kármán frequency of the stationary cylinder wake f_o is close to f_N. As U^* is varied the response of the cylinder, in particular the amplitude of oscillation, A/D, varies significantly. The forced oscillations involve a different, but generally analogous, set of parameters. The forced cylinder oscillations are typically at a constant A/D while the frequency of forced oscillation, f_e, is varied about the point where f_e/f_o equals unity. The relationship between the independent variables for the forced and free experiments is determined by assuming that the frequency of the forced oscillations is equivalent to the oscillation frequency of the free motion. Thus U^* varies inversely with f_e/f_o.

2. Experimental method

In this paper results are presented from two different sets of experiments. The forced oscillation experiments were performed in a free-surface water channel at Lehigh University, while the experiments on the elastically-mounted cylinder were conducted in the Cornell ONR Water Channel. The two sets of experiments were not specifically designed to investigate the relationship between forced and freely oscillating bodies. However, the experiments traverse very similar regions of parameter space and this fact, along with the similarity of the results, forms the basis of our comparison. For the forced oscillations the cylinder was mounted horizontally and oscillated transverse to the free-stream with a purely sinusoidal motion, such that its vertical motion was given by:

$$y(t) = A\sin(2\pi f_e t). \tag{1}$$

During each set of experiments the amplitude of oscillation was held constant, while the frequency was varied between $0.74 < f_e/f_o < 1.27$. These experiments were conducted at a number of oscillation amplitudes: $A/D = 0.25$, 0.4, 0.5 and 0.6. In the hydroelastic experiments the cylinder was mounted vertically beneath air bearings located above the channel working section. The air bearings allow the cylinder to move transverse to the free-stream such that its motion is directly analogous to the forced motion. When the motion of the elastically-mounted cylinder is synchronised with the wake the flow-induced motion is sinusoidal in nature, and is to a good approximation described by equation 1. For the forced experiments $Re = UD/\nu = 2300$ to 9100, while for the elastically-mounted case *Re* varied between 3000 and 3700. The experimental techniques and facilities are described in more detail in [7,2]. As discussed by [2], and subsequently by [5,7], the total fluid force on the oscillating cylinder can be considered as having two components: the vortex force, due to the movement of vortex structures in the wake, and the apparent mass force generated by the displacement of fluid as the body accelerates. For a cylinder oscillating transverse to the free-stream the lift force on the cylinder can be written as:

$$C_L(t) = C_{L\ \mathrm{vortex}}(t) + C_{L\ \mathrm{am}}(t), \tag{2}$$

where $C_L(t)$, $C_{L\ \mathrm{vortex}}(t)$ and $C_{L\ \mathrm{am}}(t)$ are the time varying total, vortex and apparent mass lift coefficients respectively. In general, a good approximation for the total lift force or the vortex force in the synchronization regime is given by a sinusoidal function. Govardhan and Williamson [2] introduced the concept of representing the vortex force in terms of the following expression:

$$C_{L\ \mathrm{vortex}}(t) = C_{L\ \mathrm{vortex}}\sin(2\pi f_e t + \phi_{L\ \mathrm{vortex}}), \tag{3}$$

where they defined $C_{L\ \mathrm{vortex}}$ as the vortex force coefficient, and $\phi_{L\ \mathrm{vortex}}$ as the phase of the vortex force with respect to the cylinder's displacement $y(t)$. The vortex force was then shown to be a key parameter in relating vortex dynamic modes to induced fluid forces. The classical expression for the total force is given by:

$$C_L(t) = C_L\sin(2\pi f_e t + \phi_L), \tag{4}$$

where C_L and ϕ_L are the amplitude and phase of the total lift coefficient respectively. If the total and vortex lift forces are accurately represented by Eqs. (4) and (3) then the normalised energy transfer from the fluid to the cylinder is approximated by:

$$C_E \approx \pi\frac{A}{D}C_L\sin(\phi_L) \approx \pi\frac{A}{D}C_{L\ \mathrm{vortex}}\sin(\phi_{L\ \mathrm{vortex}}). \tag{5}$$

3. Forced wake states – response at low oscillation amplitudes

When the cylinder is forced to oscillate at relatively low amplitudes two different wake states are observed. These two wake states, the "low-" and "high-frequency" states, have characteristic wake structures and force properties, as described by [7,8]. The transition between these two states corresponds to a "jump" in both the amplitude and phase of the total and vortex lift forces on the cylinder. In Fig. 1 characteristic wake structures for the low- and high-frequency states are shown using phase-averaged and mean vorticity fields. The slight asymmetry in the mean fields can be attributed to the fact that they were calculated using images from only four and two complete oscillation cycles for the low- and high-frequency states respectively. The phase-averaged images at the top of the oscillation cycle shown in Fig. 1(a&b)(i) reveal the difference in the timing of vortex shedding; the low-frequency wake is about to shed a negative vortex structure into the near wake, whilst at the same phase point in the high-frequency wake a positive vortex is about to be shed. The change in the phase of vortex shedding at the transition between these two states has been observed over a wide range of oscillation and flow parameters for cylindrical [7], and non-cylindrical bluff bodies [9].

The low-frequency wake forms long attached shear layers and typically two counter-rotating vortex pairs (defined as the "2P mode" from the forced vibration experiments of Williamson and Roshko [4]) are shed per oscillation cycle. However, for the relatively small oscillation amplitude of $A/D = 0.25$, shown in Fig. 1(a(i)), the shorter attached shear layers result in the formation of only a single vortex structure from each shear layer (2S). For frequencies above the jump the high-frequency wake, shown in Fig. 1(b(i)), is clearly different from the low-frequency wake: the attached vorticity wraps tightly around the base of the cylinder and, over the full range of A/D considered, the mode of vortex shedding was 2S. Thus, as discussed in [8], the

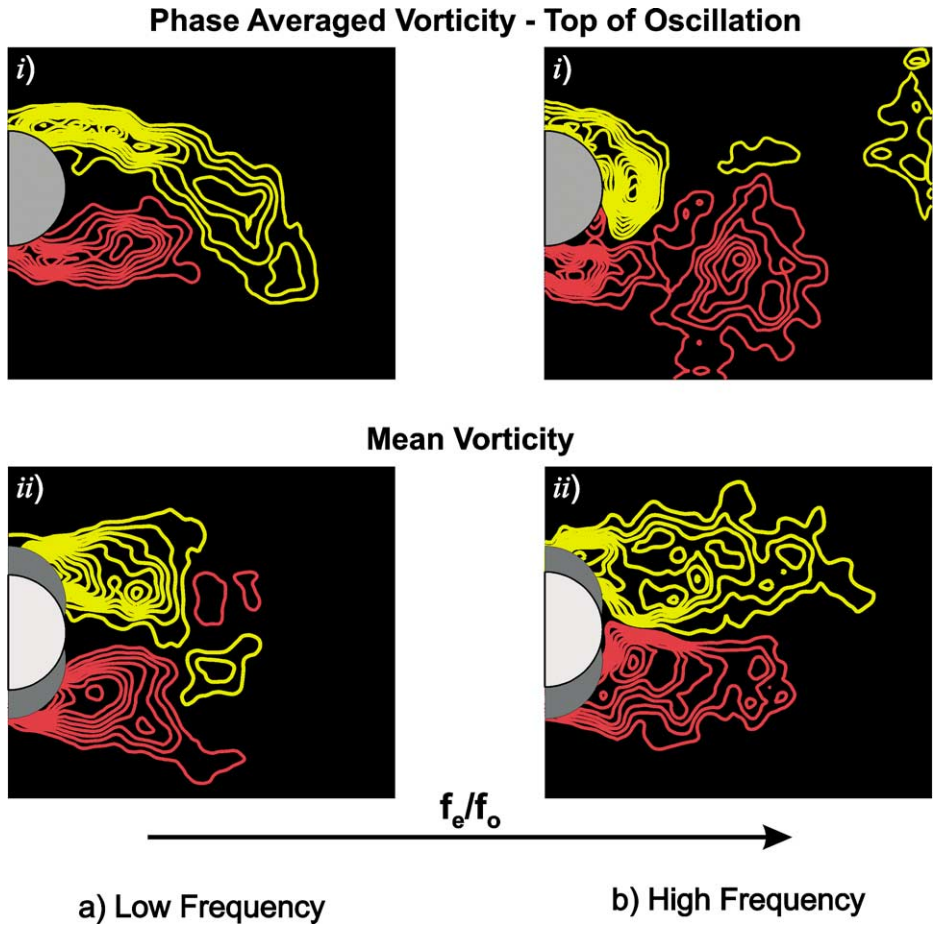

Fig. 1. Vorticity fields for forced oscillations at $A/D = 0.25$: (a) low-frequency state and (b) high-frequency state. The upper images are phase averaged fields at the top of the oscillation cycle, the lower images are mean vorticity fields calculated over a number of complete oscillation cycles.

transition between the low- and high-frequency states corresponds to a change in the mode of vortex shedding for all but the smallest values of A/D. At low oscillation amplitudes the mode of vortex shedding for both the low- and high-frequency wakes is 2S, however the mean vorticity fields, shown in Fig. 1 (a(ii)) and ((b)ii) at $A/D = 0.25$, are clearly different. Behind the main shear layer the mean low-frequency wake has small lobes of oppositely signed vorticity, whilst the mean high-frequency wake is similar to that of a stationary cylinder shown by [10]. These differences can be attributed to the change in the phase of vortex shedding, which alters the relative position of vorticity throughout the oscillation cycle.

4. Free response branches – response at high mass-damping

The amplitude response of an elastically-mounted cylinder within the synchronisation region is shown in Fig. 2 using experimental data at both low values of mass-damping, Khalak and Williamson [11], and high mass damping values, Feng [1]. The elastically-mounted cylinder displays a number of distinctly different states or response branches that, as described by [12, 13,2], exhibit characteristic force properties, oscillation amplitudes and wake structures. For cases with relatively high mass-damping there are two branches of amplitude response: the "initial" and "lower" branches. As U^* increases from zero the first response branch encountered is the initial branch, while the lower branch is found at higher U^*. As U^* varies inversely with f_e/f_o, in terms of parameter space the lower branch corresponds to the forced low-frequency state and the initial branch corresponds to the high-frequency state. Interpretations of hydrogen bubble visualizations by Khalak and Williamson [12,13] and subsequent proof, employing measurements of vorticity for the first time on this problem by Govardhan and Williamson [2], showed that the vortex shedding mode for the lower branch was generally 2P, while for the initial branch the mode of vortex shedding was 2S. These results are consistent with the corresponding low- and high-frequency states described above and with the map of wake modes produced by Williamson and Roshko [4]. Additionally, the transition between the lower and initial branches corresponds to a jump in ϕ_L of similar magnitude and direction to the jump observed between the low- and high-frequency states for the forced case.

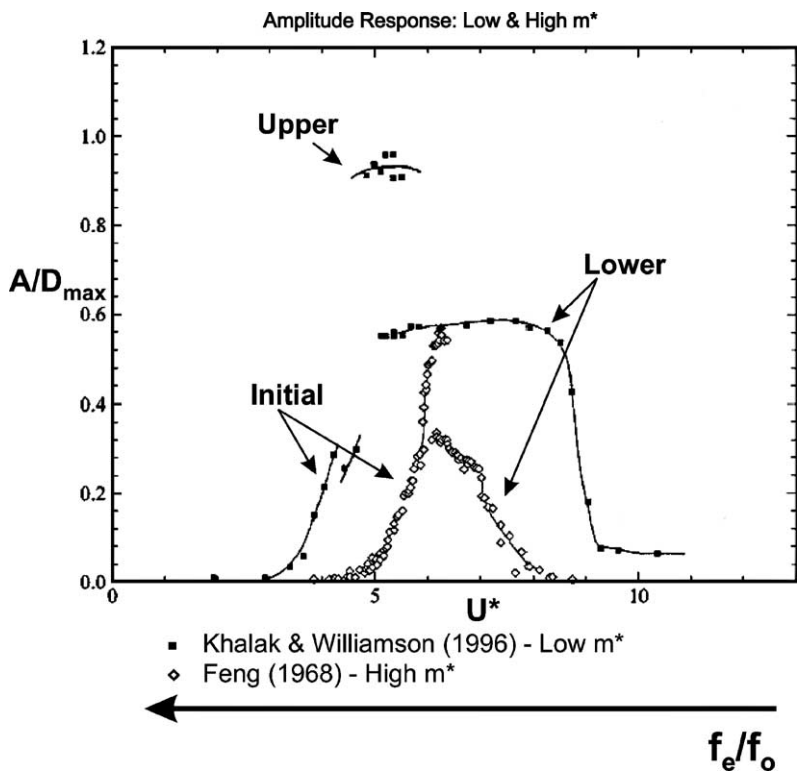

Fig. 2. The amplitude response branches for a freely oscillating elastically-mounted cylinder plotted against U^*, where U^* varies inversely with f_e/f_o. Two cases are shown low $m^*\zeta$ (Khalak and Williamson [11]) and high $m^*\zeta$ (Feng [1]).

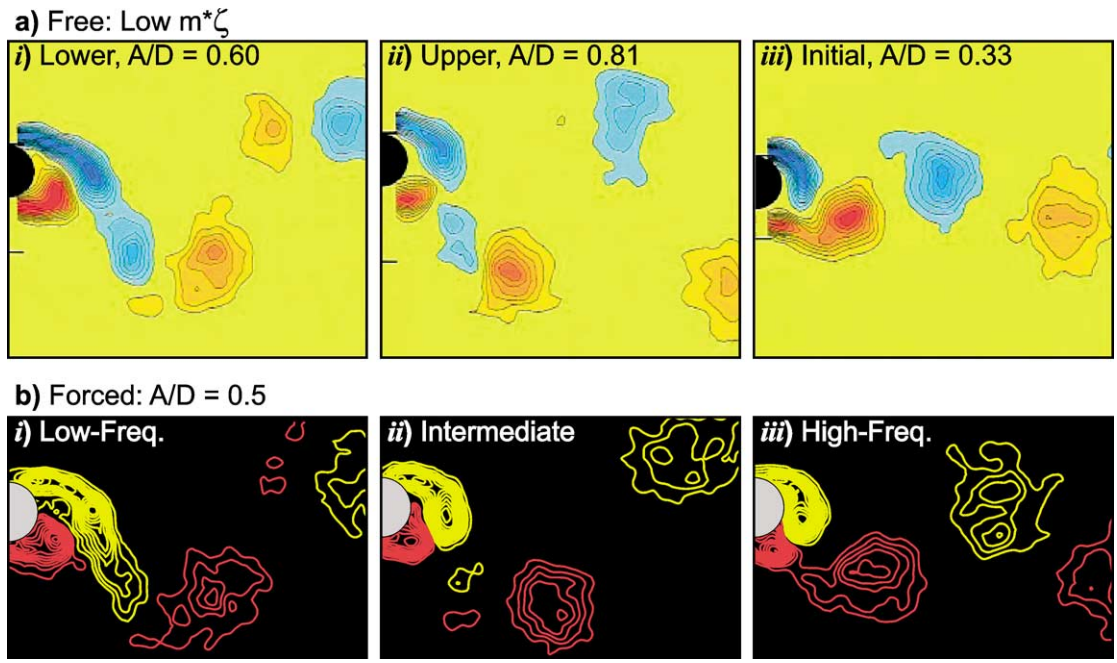

Fig. 3. Vorticity fields showing (a) the three response branches of the freely oscillating cylinder at low m^* and (b) the corresponding forced oscillation wake states at $A/D = 0.5$. (i) The lower branch and low-frequency state occur at low f_e/f_o values, (ii) the upper branch and intermediate state are observed as f_e/f_o approaches unity while (iii) the initial branch and high-frequency state occur at higher values of f_e/f_o. (f_e/f_o varies inversely with U^*.)

5. Free response branches – response at low mass-damping

The experiments of [12,13] showed that for low values of mass-damping the elastically-mounted cylinder exhibits a third "upper" response branch. As shown in Fig. 2, the upper response branch corresponds to large amplitudes of oscillation (with $(A/D)_{\max}$ typically greater than 0.7) and is found at U^* between those at which the initial and lower branches are observed. The wake structures corresponding to the lower, upper and initial branches are shown in Fig. 3(a) for a low-$m^*\zeta$ value of 0.013. At this mass-damping value the amplitude of the cylinder's response is relatively large and the upper and lower branch are shown at $A/D = 0.81$ and 0.6 respectively. As discussed above, the vortex shedding mode for the lower and initial branches are 2P and 2S respectively. The mode of vortex shedding for the upper branch is similar to that of the lower branch. However, as shown in Fig. 3(a(ii)), the second vortex in each pairing is significantly weaker than the first, although it is clear from the work of Govardhan and Williamson [2] that the vortex formation is again a 2P mode. Importantly, the phase of large scale vortex shedding for the upper and lower branches appears to be almost identical, while between the upper and initial branches there is a clear difference in the vortex shedding phase. The total and vortex lift phases for the three response branches are shown as a function of U^* in Fig. 4(a). Flow-induced motion requires positive energy transfer from the fluid to the cylinder; for the elastically-mounted cylinder $0^\circ < (\phi_L \text{ and } \phi_{L\ \text{vortex}}) < 180^\circ$. For all three of the response branches at low-m^*, the values of ϕ_L and $\phi_{L\ \text{vortex}}$ are close to either 0° or 180°. As the system moves between the three branches there is a jump of almost 180° in both ϕ_L and $\phi_{L\ \text{vortex}}$. However, the jump in ϕ_L occurs at the transition between the lower and upper branches, whereas the jump in $\phi_{L\ \text{vortex}}$ occurs at the transition between the upper and initial branches. Relating these changes to the structure of the near wake we observe that the downward jump in $\phi_{L\ \text{vortex}}$ corresponds to a change in both the mode, from 2P to 2S, and phase of vortex shedding. The jump in ϕ_L does not correspond to a significant change in the phase of vortex shedding, although there is a noticeable change in the distribution of vorticity as the second vortex in each pair becomes weaker than the first. At all these transitions there is an abrupt change in the response amplitude.

6. Forced wake states – response at high oscillation amplitudes

The results for the freely oscillating cylinder at low-m^* suggest that there might be a third forced wake state between the low- and high-frequency states. Although previous investigations have considered large amplitude forced oscillations this third wake

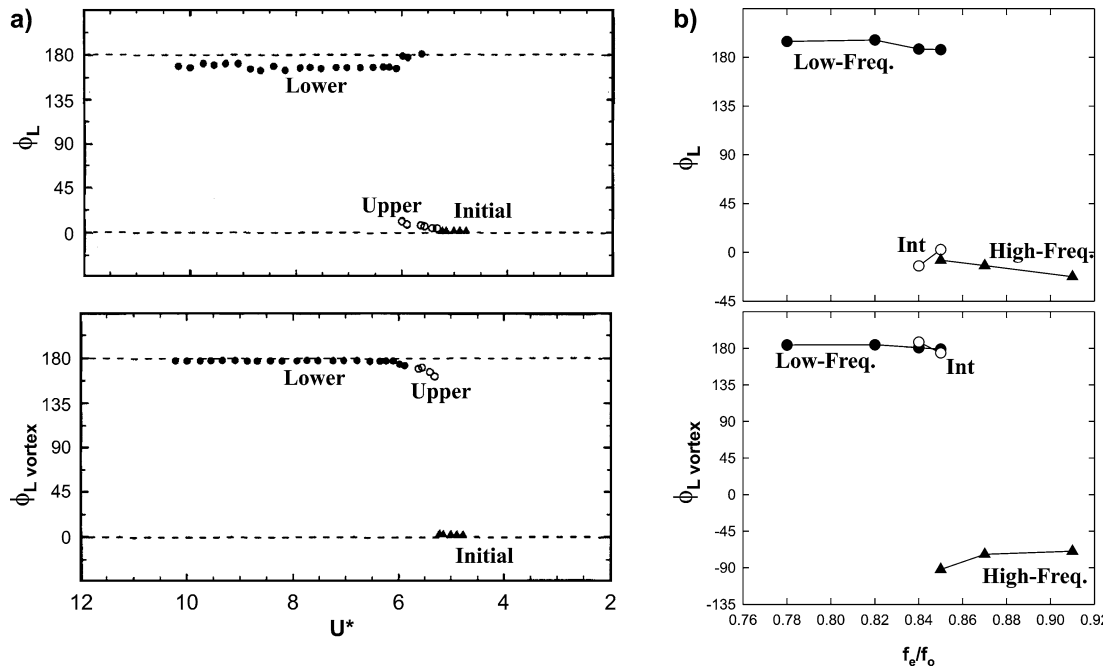

Fig. 4. Total and vortex phases for (a) the free response branches at low $m^*\zeta$ values and (b) the corresponding forced wake states at $A/D = 0.6$. Note in (a) the phases are plotted against decreasing U^*.

state was only recently identified, [5]. This third wake state is called the "intermediate" state and was observed at oscillation amplitudes of $A/D = 0.5$ and 0.6. Characteristic near wake vorticity fields for the three wake states at $A/D = 0.5$, are shown in Fig. 3(b). The characteristic features of the low- and high-frequency wakes in Fig. 3(b((i) and (iii))) are very similar to those found at lower oscillation amplitudes, where the intermediate state is not observed. As A/D increases the length of the attached shear layers increases. This is particularly evident in the low-frequency wakes and, as illustrated by comparing Figs. 1(a(i)) and 3(b(i)), can result in a change in the low-frequency mode of vortex shedding. However, the phase of vortex shedding for the low- and high-frequency states does not vary significantly as A/D increases.

The intermediate state is clearly different from both the low-and high-frequency states. Comparing the intermediate and low-frequency states the phase of vortex shedding appears similar, but the attached shear layers of the intermediate wake are much shorter and more tightly formed, resulting in the formation of a 2S wake. Comparing the intermediate and high-frequency wakes it is clear that the general mode of vortex shedding is in both cases 2S. However, the phase of vortex shedding is very different and, for the same oscillation amplitude, the intermediate wake downstream of the cylinder is much wider. Examination of the total and vortex lift phases in Fig. 4(b) shows why the presence of the intermediate state has only recently been identified. As for the elastically-mounted cylinder there is a large jump in both ϕ_L and $\phi_{L\ \mathrm{vortex}}$, with the jumps occurring at different transition points. The jump in ϕ_L occurs at the transition between the low-frequency and intermediate states, while the jump in $\phi_{L\ \mathrm{vortex}}$ occurs in between the intermediate and high-frequency states. Whereas for the elastically-mounted cylinder the existence of the upper branch is indicated by a significantly larger response amplitude, when the cylinder is forced to oscillate at a constant A/D the existence of the intermediate branch is not so clearly identified. In fact, it is not until both the total and vortex phases are simultaneously evaluated and compared, preferably in conjunction with the structures in the near wake, that the existence of the intermediate state becomes apparent.

7. Comparison between forced and free oscillations and conclusions

In this section the properties of the low-frequency, intermediate and high-frequency states are compared with the those of the lower, upper and initial branches respectively. Fig. 4 shows a strong similarity in the variation of the total and vortex lift phases for the forced and freely oscillating cylinders and in both cases the jump in $\phi_{L\ \mathrm{vortex}}$ corresponds to the jump in the phase of vortex shedding. This is physically significant as the vortex force is representative of the force due to the movement of vortex structures in the wake. The wake structures in Fig. 3 also show a very strong correlation between the phase referenced near wake structures for the corresponding forced wake states and free response branches. The results shown in Figs. 3 and 4, in

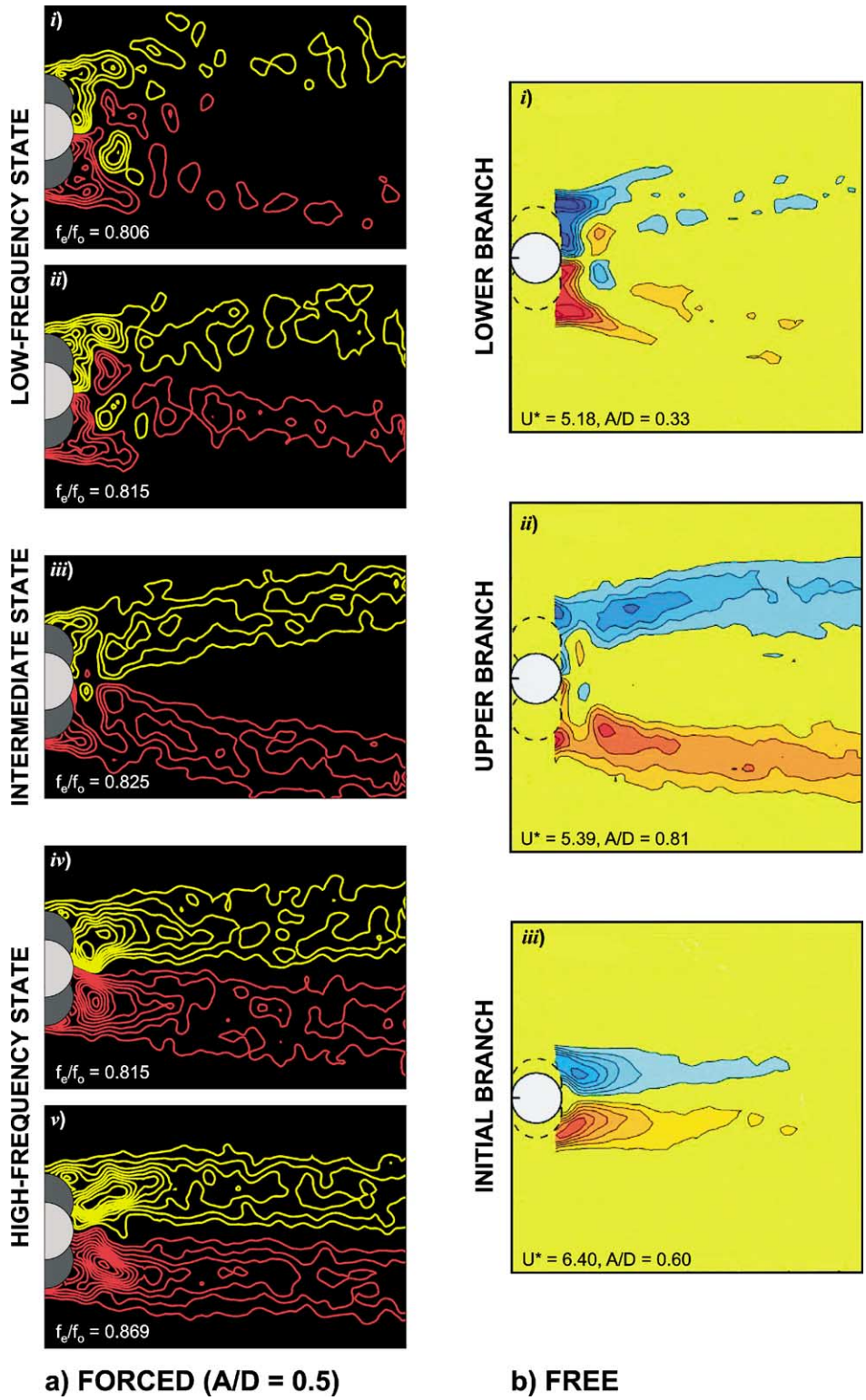

Fig. 5. Mean vorticity fields for the three wake regimes for (a) forced oscillations at $A/D = 0.5$ and (b) the freely oscillating cylinder.

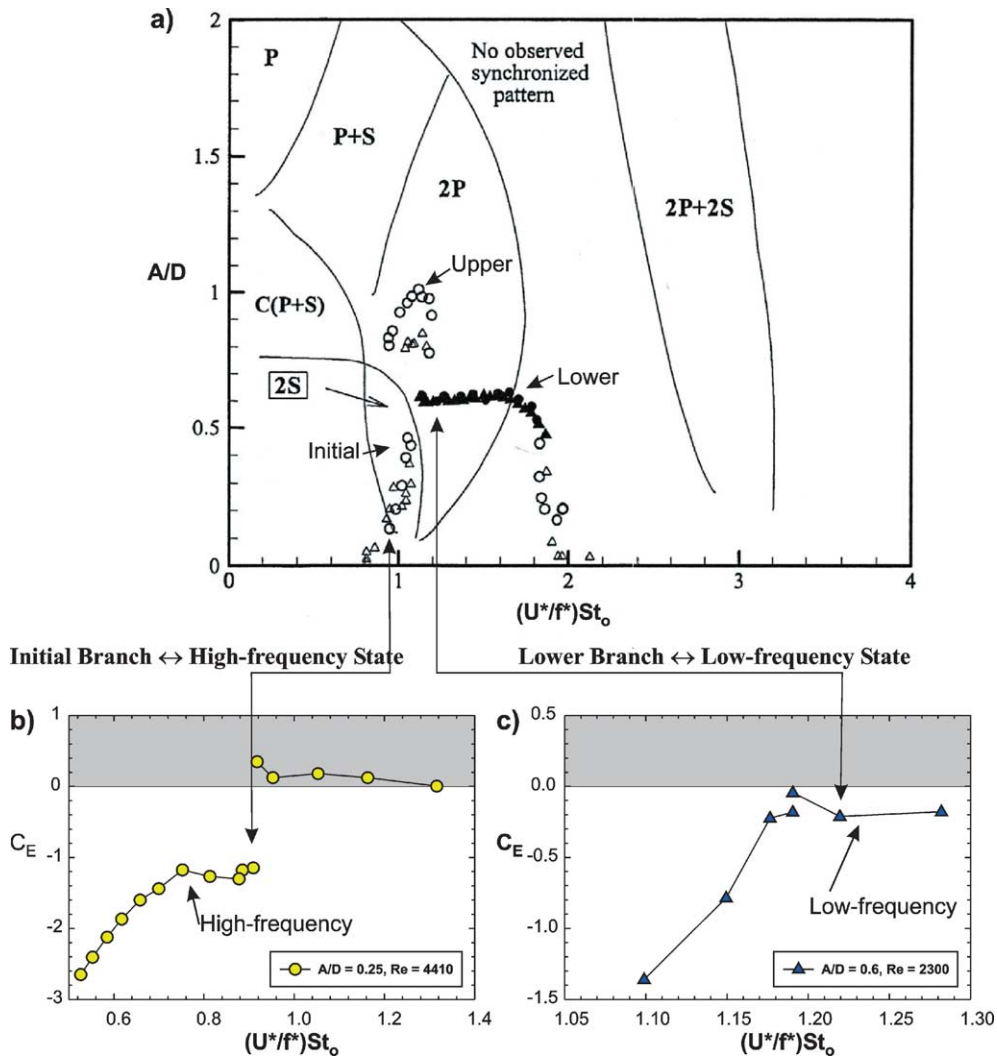

Fig. 6. (a) The response obtained by [13] for the initial and lower branches of a freely oscillating case ($m^* = 1.19$ and 8.63, $Re = 3500$–$10\,000$) are compared with the energy transfer for the forced oscillations for (b) the high-frequency state at $A/D = 0.25$ and (c) the low-frequency state at $A/D = 0.6$.

conjunction with those at lower forced oscillation amplitudes and higher-$m^*\zeta$, indicate that the forced wake states correspond to the free response branches as summarised below:

Low-Frequency State $\Longleftrightarrow$ *Lower Branch*,

Intermediate State $\Longleftrightarrow$ *Upper Branch*,

High-Frequency State $\Longleftrightarrow$ *Initial Branch*.

The relationship between the forced wake states and free response branches is further supported by the similarity of the mean vorticity fields. In Fig. 5 the mean vorticity fields for the three forced regimes are compared with the corresponding fields for the freely oscillating cylinder. The mean fields for each of the regimes are clearly different and there is a strong similarity between the mean fields for the corresponding forced and free regimes.

The mean vorticity fields for the low-frequency state and the lower branch correspond to shedding modes that at these oscillation amplitudes are clearly 2P. The mean wakes have significant regions of vorticity which have crossed the centre-line of the wake, which is indicative of the strength of the vorticity in the long shear layers extending across the base of the cylinder. The small lobes of oppositely signed vorticity downstream of the main shear layer and close to the wake centreline are similar to

those in Fig. 1(a(ii)) at $A/D = 0.25$. The mean vorticity fields for the intermediate and upper branch wakes are characterised by wide bands of positive and negative vorticity angling away from the centreline of the wake and small lobes of oppositely signed vorticity close to the wake centreline. The distributions of the mean vorticity for both the forced and freely oscillating cases are very similar despite the differences in A/D, and the fact that the vortex shedding mode for the upper branch is weakly 2P, while the intermediate wake is 2S. The mode of vortex shedding for the high-frequency and initial branch wakes is 2S and the mean vorticity fields are very narrow. Interestingly, the mean fields for the low-frequency state, intermediate state, lower branch and upper branch all exhibit small lobes of oppositely signed vorticity near the wake centreline and all have a similar phase of large scale vortex shedding. The vortex shedding phase for both the high-frequency state and the initial branch is distinctly different and this small lobe of vorticity is not present.

The forced purely sinusoidal oscillations appear to reproduce the different wake structures and lift phases observed for a freely oscillating cylinder. This indicates that the forced oscillations are simulating many of the important features of the flow-induced motion. The variation of ϕ_L and $\phi_{L\ \mathrm{vortex}}$ presented in Fig. 4 are remarkably similar. However, many of the values of ϕ_L and $\phi_{L\ \mathrm{vortex}}$ for the forced oscillations are outside the region of positive energy transfer, $0^\circ < (\phi_L \text{ and } \phi_{L\ \mathrm{vortex}}) < 180^\circ$, and therefore predict that flow-induced motion would in fact not occur.

Fig. 6 shows a comparison of the energy transfer for forced oscillations with the response of a freely oscillating cylinder, where by definition the energy transfer for the free case must be positive. The amplitude response of the freely oscillating cylinder plotted against $(U^*/f^*)St_o$ in Fig. 6(a) shows a good collapse for both the initial and lower branches. In Fig. 6(b) and (c) the energy transfer for the forced oscillations are also plotted as a function of $(U^*/f^*)St_o$ at $A/D = 0.25$ and 0.6 respectively. For values of $(U^*/f^*)St_o$ between 1.19 and 1.29 the energy transfer coefficient for the low-frequency state at $A/D = 0.6$ and $Re = 2300$ is negative. However, Fig. 6(a) shows that for values of $(U^*/f^*)St_o$ between 1.1 and 1.6 lower branch flow-induced vibrations occur at $A/D = 0.6$ for a similar Reynolds number of $Re = 3700$. Similarly, for the free initial branch at $(U^*/f^*)St_o$ of just below 1 free oscillations occur at $A/D = 0.25$. However, the high-frequency state forced oscillations at this amplitude and similar values of $(U^*/f^*)St_o$ result in negative energy transfer.

These results show that although the forced purely sinusoidal oscillations replicate many features of the flow-induced motion they can result in negative energy transfer for flow and oscillation parameters where free oscillations are known to occur. In these cases, the forced sinusoidal motion cannot predict the flow-induced motion and therefore, the sinusoidal motion does not simulate all the key components of the flow-induced motion. The experimental results presented here were obtained in two separate facilities. Further work using a co-ordinated approach, in particular careful matching of Re and A/D, is clearly needed to reconcile the difference in the sign of the energy transfer with the good agreement between the flow fields in the forced and freely oscillating cases.

References

[1] C. Feng, The measurements of vortex-induced effects in flow past a stationary and oscillating circular and d-section cylinders, Master's thesis, University of British Columbia, Vancouver, BC, Canada, 1968.
[2] R. Govardhan, C. Williamson, Modes of vortex formation and frequency response of a freely vibrating cylinder, J. Fluid Mech. 420 (2000) 85–130.
[3] T. Sarpkaya, Vortex induced oscillations – a selective review, ASME J. Appl. Mech. 45 (1979) 241–258.
[4] C. Williamson, A. Roshko, Vortex formation in the wake of an oscillating cylinder, J. Fluids Structures 2 (1988) 355–381.
[5] J. Carberry, J. Sheridan, D. Rockwell, Controlled oscillations of a cylinder: a new wake state, J. Fluids Structures (2003) in press.
[6] T. Staubli, Calculation of the vibration of an elastically mounted cylinder using experimental data from forced oscillation, J. Fluids Engrg. 105 (1983) 225–229.
[7] J. Carberry, J. Sheridan, D. Rockwell, Controlled oscillations of a cylinder: forces and wake modes, J. Fluid Mech. (2003) in press.
[8] J. Carberry, J. Sheridan, D. Rockwell, Forces and wake modes of an oscillating cylinder, J. Fluids Structures 15 (2001) 523–532.
[9] T. Staubli, D. Rockwell, Pressure fluctuations on an oscillating trailing edge, J. Fluid Mech. 203 (1989) 307–346.
[10] R. Govardhan, C. Williamson, Mean and fluctuating velocity fields in the wake of a freely-vibrating cylinder, J. Fluids Structures 15 (2001) 489–501.
[11] A. Khalak, C. Williamson, Dynamics of a hydroelastic cylinder with very low mass and damping, J. Fluids Structures 10 (1996) 455–472.
[12] A. Khalak, C. Williamson, Fluid forces and dynamics of a hydroelastic structure with very low mass and damping, J. Fluids Structures 11 (1997) 973–982.
[13] A. Khalak, C. Williamson, Motions, forces and mode transitions in vortex induced vibrations at low mass-damping, J. Fluids Structures 13 (1999) 813–851.